

1 **Author Accepted Manuscript (AAM)**

2 This document is the Author Accepted Manuscript (AAM) of the following article:

3

4 A large closed canopy chamber for measuring CO<sub>2</sub> and water vapour exchange of  
5 whole trees

6 Oscar Pérez-Priego<sup>a,\*</sup>, Luca Testi<sup>a,b</sup>, Francisco Orgaz<sup>a</sup>, Francisco J. Villalobos<sup>a,b</sup>

7

8 <sup>a</sup>Instituto de Agricultura Sostenible (IAS), Consejo Superior de Investigaciones Científicas (CSIC), Alameda del Obispo, s/n, 14004 Córdoba, Spain

9 <sup>b</sup>Dpto. de Agronomía, Universidad de Córdoba, Spain

10

11 The final published version (Version of Record) is available at:

12 doi:10.1016/j.envexpbot.2009.10.009

13

14 This manuscript is distributed in accordance with Elsevier's self-archiving policy.

15

16

17 **Abstract**

18 A transient-state chamber was developed to measure canopy gas exchange of single trees in  
19 the field. The chamber, with a volume of 41.6 m<sup>3</sup>, is designed to enclose a medium-size  
20 orchard tree; chamber top and windows can be left open, causing minimum disturbance to the  
21 tree environment. Transitory closures allow simultaneous measurement of CO<sub>2</sub> exchange and  
22 transpiration of the enclosed tree. The chamber was tested during a 2-year study in an olive  
23 orchard submitted to different irrigation treatments: control with no water stress (CI) and  
24 regulated deficit irrigation (RDI). Leakage had a minimal impact on flux calculations  
25 (0.8%min<sup>-1</sup>); adsorption was not detectable. Maximum increases in canopy temperature of  
26 0.58°Cmin<sup>-1</sup> for CI and 1.3°Cmin<sup>-1</sup> for RDI generated very small effects on fluxes.  
27 Changes in the transpiration rate induced by the chamber's modification of the canopy  
28 environment were evaluated by continuous sap flow measurements with heat pulse gauges  
29 inserted in the trunk of two trees enclosed by chambers. Results showed a sap flow decrease  
30 of about 8% after 180 s of chamber closure. The artificial turbulence generated by fans into  
31 the chamber to facilitate air mixing did not alter the transpiration rate. The enclosure had a  
32 very small impact on the tree canopy conductance (G<sub>c</sub>). The initial lag and mixing time was  
33 estimated as 30 s; the optimal duration of the calculation window was 70 s. Hourly carbon  
34 assimilation (A), transpiration (E), and water use efficiency (WUE) for two olive trees in the  
35 field subjected to different levels of water stress were measured.

36 **Keywords:** Canopy chamber Canopy gas exchange Carbon balance Carbon assimilation  
37 Water use efficiency Water stress, *Olea europaea* L.

38

39

## 40 Introduction

41 The measurement of carbon assimilation and water use of trees is critical to understand the  
42 processes leading to their carbon and water balance, but is difficult to perform at the whole-  
43 plant level. At leaf level, cuvette gas analysers have been used to measure leaf gas exchange  
44 of mature trees (e.g. Moriana et al., 2002). Scaling up such observations to canopy level,  
45 however, remains a challenge. A suitable method for measuring the gas exchange of  
46 individual trees is the use of large canopy chambers. Nevertheless, there are practical  
47 difficulties in the design, construction and operation of chambers large enough to enclose a  
48 whole tree. Denmead (1984) classified gas exchange canopy chambers into open (steady-  
49 state) and closed (transient-state) systems. The open system continuously renews the air  
50 inside the chamber while measuring the gas concentration in the entry and exit airstreams.  
51 This type of chamber is always closed and under constant forced ventilation, thus the  
52 radiative and aerodynamic microclimate around the tree can be very different from the  
53 natural undisturbed conditions.

54 In most open chamber systems with air supply, there is a constant overpressure within the  
55 chamber to keep the structure inflated. Furthermore, steady airflow is often higher than  
56 natural wind speed and a suitable ventilation rate is difficult to get. A large air-pumping  
57 system with high electrical power is required (Greenwood et al., 1981; Denmead, 1984).  
58 Another critical aspect is the radiation environment in the chamber. The walls alter the  
59 radiation amount and quality inside the chamber, by reducing direct beam solar radiation and  
60 increasing the diffuse component (Leuning and Foster, 1990). Although this problem is  
61 common to all chamber types, it has a bigger effect in open chambers due to the permanent  
62 placement of the enclosure during the measurement period. Enclosing a canopy into a  
63 chamber always generate important microclimatic differences between the chamber and the  
64 environment (Denmead et al., 1993), thus the enclosing time should be as short as possible.

65 Transient-state closed chambers are closed for a short period of time (min), while the change  
66 in gas concentration is measured. They are portable and can be placed on the plant for the  
67 measurement; they are then removed before the plant can respond physiologically to the  
68 changing environment. Reicosky and Peter (1977) described this type of easily moving  
69 chambers for measuring transpiration on field plots. More recently, this type of canopy  
70 chamber has been automated for continuous measurements of CO<sub>2</sub> and H<sub>2</sub>O fluxes (Steduto  
71 et al., 2002). The simplest method for calculating gas fluxes with a closed chamber is by  
72 performing a linear regression of gas concentration with time. The principles involved in this  
73 approach have been reviewed by Jarvis et al. (1971). Later, different methods of calculation  
74 have been proposed by Reicosky et al. (1990) and Wagner et al. (1997). Wagner and  
75 Reicosky (1992) studied the chamber effect on the plant environment, measuring changes in  
76 canopy photosynthesis rates and evapotranspiration rates. The relevant factors involved are  
77 mostly CO<sub>2</sub> and water vapour concentration, canopy temperature, air temperature, canopy  
78 boundary layer conductance, stomatal conductance (g<sub>l</sub>) and vapour pressure deficit (VPD).

79 Researchers mostly used small closed chambers on plants or pots (Reicosky and Peter, 1977;  
80 Reicosky, 1990a, 1990b; Held et al., 1990; Pickering et al., 1993; Grau, 1995; Steduto et al.,  
81 2002; McLeod et al., 2004). Most transitory-closed chambers not exceeding 9 m<sup>3</sup> in volume  
82 are reported in the literature, used mainly on herbaceous crops. Most of them have been  
83 evaluated comparing with accurate and direct methods such as a weighing lysimeter  
84 (Reicosky et al., 1983; Pickering et al., 1993) and heat pulse sap flow (Dragoni et al., 2005)  
85 or micrometeorological methods (Held et al., 1990; Dugas et al., 1991; Steduto et al., 2002;

86 McLeod et al., 2004). Enclosing trees with a canopy size larger than 20 m<sup>3</sup> has not yet been  
87 tried in a closed system design. A possibility is to use a frame structure, relatively easy to  
88 move, which can be opened and closed through revolving top and windows. Such a chamber  
89 should ideally disturb minimally the tree environment while open.

90 The objectives of this work were: (a) to design a chamber of the transitory-closed type, large  
91 enough to enclose adult orchard trees; (b) to test the chamber for measuring canopy gas  
92 exchange in the field, and (c) to evaluate physical and physiological responses of the tree to  
93 potential environmental modifications of the chamber.

## 94 **2. Materials and methods**

### 95 *2.1. Chamber description*

96 The transient-state closed chamber presented here is a variation of the chamber described by  
97 Reicosky and Peter (1977), compatible for simultaneous measurement of both CO<sub>2</sub> and water  
98 vapour exchange. The chamber consists of a hexagonal prism with base of 10.4 m<sup>2</sup> and  
99 height of 4 m; the volume – 41.6 m<sup>3</sup> – is enough to enclose a mature tree of most of the  
100 cultivated fruit species (Fig. 1). The walls are assembled with 12 sections of rigid aluminium  
101 frames (2 m × 2 m) that are easy fitted and screwed together. The whole chamber is mounted  
102 around the tree on a firm stainless steel frame with sharp supports sunk in the soil. The  
103 bottom is sealed around the tree trunk through a thick polyethylene panel; thus, fluxes from  
104 the soil are excluded. The top is made by two trapezium-shaped windows. The top and four  
105 of the six walls are hinged windows, which allow quick opening and closing operation.  
106 Windows and tops are made of Llumar® “NRS90 clear” polyester film of 75 μm thickness,  
107 stretched and fixed to the aluminium frames; this film was chosen for its excellent broadband  
108 transmittance. The top and upper windows can be quickly moved manually by extended  
109 handles. The chamber contains four 80 W fans of 40 cm diameter attached to the basal frame,  
110 mixing the air inside the chamber during the closed period (which in normal operating  
111 conditions does not need to exceed three minutes). A vacuum pump circulates the air through  
112 the sampling circuit: the air is taken from inside the chamber through many intake points,  
113 spatially distributed through the chamber volume (Fig. 1) and is then returned to the chamber.  
114 A sample of 1 L min<sup>-1</sup> of this air flow is sniffed using a small pump and diverted to a CO<sub>2</sub>  
115 /H<sub>2</sub>O infrared gas analyser (IRGA) (model LI-COR LI-840, Lincoln, NE, USA) which  
116 measures CO<sub>2</sub> and water vapour concentrations simultaneously at 1 Hz sampling rate; the  
117 output is recorded by a datalogger (model CR23X, Campbell Scientific, Logan, UT, USA).  
118 The IRGA, datalogger and small pump were powered by 12 V batteries. The vacuum pump  
119 and the fans are powered using a small portable A/C generator.

120 An infrared thermometer (model IRTS-P, Apogee, UT, USA) is mounted on the centre of the  
121 chamber top, facing downwards, to measure the temperature of the canopy. The sensor has a  
122 52° field of view, and can be aimed and adjusted in height for optimal foliage targeting. The  
123 air temperature and relative humidity were measured inside the chamber with a combined  
124 probe (model CS215, Campbell Scientific, Logan, UT, USA) placed near the top of the  
125 chamber into a radiation shield. Air temperature and relative humidity were recorded every  
126 4 s in order to evaluate changes in vapour pressure deficit (VPD) in the confined atmosphere.  
127 Two complete chambers were built and arranged for simultaneous measurements in two  
128 trees.

129 The chamber is normally kept with all the windows and top in the open position. Just before  
130 measuring, the windows and top are closed and fans are turned on. The CO<sub>2</sub> and water  
131 vapour concentrations, measured by the IRGA, change steadily after a short lag time. The  
132 rate of change of both gases with time is the apparent flux of assimilation and transpiration,  
133 respectively, of the tree. The gas fluxes are transformed to mass basis per surface and time  
134 unit, simultaneously, following Jarvis et al. (1971), and include the correction for air  
135 temperature and atmospheric pressure inside the chamber (Reicosky et al., 1990). The  
136 method and calculation window used for assessing CO<sub>2</sub> exchange and transpiration rates  
137 are discussed later. After the measurement is completed, the chamber goes back to the open  
138 position, with the fans off until the following measurement.

## 139 2.2. Chamber tests

140 A series of experiments were carried out in the laboratories of the Instituto de Agricultura  
141 Sostenible (IAS) of Córdoba, Spain, to assess the potential measurement errors. Three tests  
142 were aimed to quantify some potential disturbances that the closed chamber could cast over  
143 the internal environment, namely: (a) gas leakage; (b) gas adsorption by the chamber walls  
144 and elements and (c) alteration of internal radiation levels by walls and frames. In addition,  
145 two field tests were designed to assess the magnitude of some unwanted effects that the  
146 confined environment could carry over the physiology of the enclosed canopy, in particular:  
147 (a) effect over the foliage temperature and (b) effect over the transpiration rate and the  
148 canopy conductance. These field tests were conducted in an irrigated olive (*Olea europaea* L.  
149 ‘Arbequino’) orchard planted in summer 1997 with a 3.5m×7m spacing, located in Córdoba,  
150 Spain (37.85° N, 4.8° W, altitude 110 m). Two trees in different water conditions (one from  
151 an irrigated control treatment labelled as CI and one – water stressed – from a regulated  
152 deficit irrigation treatment labelled as RDI) were chosen to test the chamber effect on  
153 physiology; two chambers, sharing the same IRGA, were mounted around these trees,  
154 allowing quasi-simultaneous operations. The Plant Leaf Area of the trees was measured using  
155 a Plant Canopy Analyser (model LAI2000, LI-COR, Lincoln, NE, USA).

156 For all tests, the IRGA was operated in the range of ±1000 μmol mol<sup>-1</sup> for CO<sub>2</sub> and ±80  
157 mmol mol<sup>-1</sup> for water vapour. A two-point calibration procedure was carried out in the  
158 laboratory before measurements operations. A weather station, located less than 300m from  
159 the experimental plot provided additional meteorological data.

160 A chamber operating as a closed system has to ensure that the envelope is tightly sealed, as  
161 leakages would alter the rate of change of the sampled gases inside the chamber. The leakage  
162 test for CO<sub>2</sub> was performed by injecting an amount of CO<sub>2</sub> into the empty chamber. The  
163 decline in [CO<sub>2</sub>] was then measured for 24 min. The leakage error was deduced from the  
164 differential equation:

$$165 \frac{dC_i}{dt} = \frac{-\theta(C_i - C_a) + F}{V} \quad (1)$$

166 where  $\theta$  is the leakage coefficient (m<sup>3</sup> s<sup>-1</sup>, specific of a given chamber),  $C_i$  and  $C_a$  the  
167 CO<sub>2</sub> concentrations inside and outside the chamber, respectively (μmolCO<sub>2</sub> mol<sup>-1</sup>),  $V$  the  
168 chamber volume (m<sup>3</sup>), and  $F$  is the assimilation ( $F < 0$ ) or respiration ( $F > 0$ ) flux (μmol CO<sub>2</sub>  
169 mol<sup>-1</sup> m<sup>3</sup> s<sup>-1</sup>). Thus, considering  $F = 0$  (empty chamber) and integrating time  $t_1$  to  $t_2$  (s),  
170 the leakage coefficient (m<sup>3</sup> s<sup>-1</sup>) is:

171 
$$\theta = \frac{-V}{\Delta t} \ln \left( \frac{C_{i2} - C_a}{C_{i1} - C_a} \right) \quad (2)$$

172 Combining F and  $\theta$  from the differential equation:

173 
$$F = -\theta(C_i - C_a) + V \frac{dC_i}{dt} \quad (3)$$

174 where the first term on the right of Eq. (3) represents the error and the second term the apparent  
175 flux (F'). Hence, for an interval time  $\Delta t$  and if  $C_{i1} \approx C_a$ , the relative error ( $\epsilon$ ) will be:

176 
$$\epsilon = \frac{-\theta(C_i - C_a)}{-\theta(C_i - C_a) + F'} = \frac{\theta \Delta t}{2V} \quad (4)$$

177 The relative error is thus not dependent on the concentration gradient, but only on the duration  
178 of the closure period. We assume that under field conditions (with non-zero wind outside and  
179 the fans on) the leakage is mainly an airflow rather than a diffusive process, thus the relative  
180 error is assumed to be equally valid for water vapour.

181 The relative error is thus not dependent on the concentration gradient, but only on the duration  
182 of the closure period. We assume that under field conditions (with non-zero wind outside and  
183 the fans on) the leakage is mainly an airflow rather than a diffusive process, thus the relative  
184 error is assumed to be equally valid for water vapour.

### 185 2.2.2. H2O adsorption and radiation transmissivity tests

186 The potential error due to H2O adsorption on the chamber walls and in the sampling tubing was  
187 evaluated by injecting a known mass of water vapour generated with a conventional humidifier  
188 machine into the closed chamber, then measuring the water vapour concentration after one  
189 minute. The test was repeated 12 times, injecting different amounts of water vapour. As the  
190 leakage flow was already known from the leakage test, the adsorbed mass was estimated as  
191 difference between the measured mass flow and the leakage flow.

192 Concurrent measurements of solar radiation inside and outside the chamber were performed  
193 to determine the attenuation of the solar radiation with the change in sun angle. Eight  
194 measurements were taken at different hours on a clear-sky day, using with a red/far red sensor  
195 (model SKR-110, Skye Instruments, UK), sensible to the wavelengths of 660 and 730 nm. The  
196 average value for the attenuation of the solar radiation by the Llummar® film resulted in 9.9%  
197 and 14.6% in the wavelengths 660 and 730 nm, respectively. The transmissivity of the chamber  
198 to the total photosynthetically active radiation (PAR) measured by a quantum meter (model  
199 QMSW-SS, Apogee Instrument Inc., Logan, UT, USA) resulted 90% in average during a clear-sky  
200 day.

### 201 2.2.3. Canopy and air temperature increase

202 Perhaps the main difficulty associated with transient closed chambers is that they are expected  
203 to increase quickly the canopy and internal air temperature by reducing convection and  
204 decreasing the long-wave radiation loss: consequently the foliage gas exchange may depart

205 from natural conditions. The infrared ther- mometer installed permanently on the chamber top  
206 permitted to monitor closely the canopy temperature, while the temperature and VPD of the  
207 stirred air inside the chamber was measured by the combined air temperature and humidity  
208 probe. Due to the effect of transpirational cooling, the temperature of the enclosed canopy  
209 varies also with the transpiration rate. For this reason, the data were collected quasi-  
210 simultaneously in both water stressed and unstressed trees. Data of air and canopy  
211 temperature increase for 175 standard chamber operations in the field (closing, measur- ing  
212 during about three minutes and unclosing) were collected in different environmental  
213 conditions, from July to October 2007.

#### 214 *2.2.4. Comparison with heat pulse sap flow*

215 This test was aimed to find out if the enclosure of the canopy into the chamber would have a  
216 significant effect on the tree transpira- tion rate, due to the general alteration of the canopy  
217 environment. The sap flow velocity was measured using heat pulse gauges inserted in the trunk  
218 of an olive tree where the chamber had previ- ously been mounted. The heat pulse velocity  
219 measurements were taken at 3-min intervals, from 09:30 to 12:30h on 5 July 2007, obtaining a  
220 quasi-continuous trace of sap velocity; at the same time the chamber was operated (closed) in  
221 periods of different duration (from about 252 to 464 s). The sap flow sensors were designed in  
222 the IAS laboratory. Each sensor consisted of three stainless steel needles of 2-mm diameter: a  
223 4.8 W heater and two temperature probes. The temperature probes were inserted into the trunk  
224 at a distance of 10- and 5-mm down- and up- stream from the heater, respectively. Each  
225 temperature probe contained 4 Type E (chromel-constantan) thermocouple junctions, spaced  
226 10mm along the needle, which were sampled independently to obtain heat pulse velocities at 4  
227 depths. Further details on the sap flow system may be found in Testi and Villalobos (2009).

#### 228 *2.3. Duration of the calculation window and gradient effect*

229 Before the exchange flux of a gas can be reflected by the rate of change of its concentration in  
230 the confined atmosphere, there is always a lag time (the time for the gas to reach the sensing  
231 chamber of the IRGA through the sampling tubing) and a stirring time (the time needed for the  
232 fans to break the leaves boundary layer and mix the confined atmosphere effectively). The  
233 combination of lag and stirring time was evaluated by injecting a pulse of CO<sub>2</sub> inside the empty  
234 chamber, and then monitoring the CO<sub>2</sub> concentration until a stable rate of change (only  
235 depending on leakage) was reached. This point was considered the beginning of the calculation  
236 window (the period of time which measurements are then actually used to calculate the flux).

237 In principle, transient-state chambers induce modifications in the internal environment right  
238 after closing. Apart from the possi- ble thermal and aerodynamic effects over the canopy, the  
239 variation itself in the concentration of the gases inside the chamber reduces the gradient  
240 between the leaves and the sampled atmosphere: the effect is that the process under study  
241 (either transpiration or photo- synthesis/respiration) is deviated from the undisturbed rate. Even  
242 keeping every other factor unchanged, the rate of change of the gas concentration vs. time is  
243 unlinear, because of gradient variation. Ideally, the undisturbed rate of gas exchange is the  
244 initial slope of this unlinear relation.

245 The concentration regression (CR) method calculates the changes of gas concentration (CO<sub>2</sub> or  
 246 water vapour) as the slope of the least squares regression line relating gas concentration to  
 247 time (Meyer et al., 1987), thus ignores the nonlinearity. On the contrary, the quadratic  
 248 regression (QR) model proposed by Wagner et al. (1997) adds a second-order term (observer  
 249 effect), and was used to account for the influence of the physical disturbances that result in  
 250 nonlinear gas concentration change inside of closed systems. The quadratic model used was:

251

252 [CO<sub>2</sub> or water vapor] = linear process + observer effect

$$253 \quad \quad \quad = a + bt + ct^2 \quad \quad [5]$$

254 The change of CO<sub>2</sub> and water vapour concentration vs. time will be:

$$255 \quad [CO_2 \text{ or water vapor}] / dt = b + 2ct \quad [6]$$

256 where b and c are the regression coefficients of the quadratic function. Then, for time zero, the  
 257 slope (which is the exchange rate unaffected by chamber closure) is simply equal to b. The  
 258 quadratic regression deals with the error of gradient reduction, but at the price of ascribing a  
 259 paramount importance to the determination of the time zero, because only the slope in this  
 260 point is the sought gas exchange rate.

261 The optimal duration of the calculation window was obtained empirically, by testing the  
 262 stability in the rate of change of the sampled gas concentration with time. The test consisted  
 263 in comparing the CR method with the QR method for 175 field measurements obtained in 2006  
 264 and 2007 in olive trees in different water status.

#### 265 *2.4. Canopy conductance approach*

266 A simplified approach for calculating canopy conductance ( $G_c$ ) in a well-ventilated canopy  
 267 chamber is the inversion of the “imposed evaporation” Penman-Monteith Equation (e.g.  
 268 Villalobos et al., 2000; Orgaz et al., 2007). Thus, canopy conductance  $G_c$  ( $m\ s^{-1}$ ) is:

$$269 \quad G_c = \frac{\gamma}{\rho C_p} \frac{\lambda E}{VPD} \quad (7)$$

270 where  $\gamma$  is the psychrometric constant ( $kPaK^{-1}$ ),  $C_p$  the specific heat capacity of air at constant  
 271 pressure ( $kJkg^{-1} K^{-1}$ ),  $\rho$  the air density ( $kg\ m^{-3}$ ),  $VPD$  the vapour pressure deficit ( $kPa$ ),  $\lambda$  is the  
 272 specific heat of vapourisation ( $MJ\ kg^{-1}$ ) and  $E$  is the transpiration rate ( $kg\ m^{-2}\ s^{-1}$ ).

273 Changes in  $G_c$  may be evaluated continuously during the measurement combining Eqs. (6)  
 274 and (7) with the rate of change of water vapour concentration and  $VPD$  vs. time:

$$275 \quad G_c = \frac{\gamma}{\rho C_p} \frac{\lambda(b + 2ct)}{VPD} \quad (8)$$

276 where b and c were already defined.

277 **3. Results**

278 *3.1. Leakage and adsorption tests*

279 The amount of CO<sub>2</sub> injected into the chamber produced an increase of 90  $\mu\text{mol CO}_2 \text{ mol}^{-1}$  .  
280 The decline in [CO<sub>2</sub>] was then measured for 24 min with the IRGA (Fig. 2). The concentration  
281 trace was divided into intervals of 2 min and leakage coefficients were calculated for each  
282 interval using Eq. (2). The mean leak coefficient calculated for all intervals resulted 0.011 m<sup>3</sup>  
283 s<sup>-1</sup> (Fig. 2). The average relative error ( $\epsilon$ ) due to leakage in the calculation of fluxes (Eq. (4))  
284 was 0.8% min<sup>-1</sup> .

285 The amount of water vapour injected with a humidifier varied from 13.8 to 91.1 g. Those water  
286 vapour injections increased the [H<sub>2</sub>O] of the chamber from 0.45 to 3.04 mmol H<sub>2</sub>O mol<sup>-1</sup>. The  
287 IRGA measured very accurately the amounts of water vapour added to the chamber (Fig. 3); no  
288 significant deviation from the 1:1 line possibly due to adsorption was observed, in the explored  
289 range.

290 *3.2. Effect on canopy and air temperature*

291 Fig. 4 represents the rate of change, during the closure operation, of the enclosed canopy  
292 temperature (Fig. 4a) and air temperature inside the chamber (Fig. 4b) vs. the free air  
293 temperature registered at the weather station nearby. The most significant increases in  
294 canopy temperature were appreciated in trees under water stress (RDI treatment) during the  
295 hot season. The maximum canopy temperature increases resulted 0.58 °C min<sup>-1</sup> in the well-  
296 irrigated control (5 July 2007, 09:00 h) and 1.3 °C min<sup>-1</sup> in the RDI (6 September 2007, 13:00  
297 h). The higher increments were observed during the hot season with high VPD in the afternoon  
298 (Fig. 4a). On the contrary, the internal air temperature rate of increase seems independent from  
299 the tree water status (Fig. 4b); also, the free air temperature affects weakly the rate of increase  
300 of the air inside the chamber. In general, the air inside the closed chamber heats up slowly: the  
301 average air temperature increases were 0.22 and 0.14 °C min<sup>-1</sup> for CI and RDI, respectively.  
302 The maximum values were found close to 0.7 °C min<sup>-1</sup> , for both treatments, recorded on 2  
303 August.

304 *3.3. Effect on transpiration rate*

305 The velocity of the sap through the xylem vessels is proportional to the transpiration flux, if the  
306 trunk diameter and capacitance do not change; thus, in the short term, variations in the sap  
307 velocity are assumed to be proportional to variations in the transpiration rate. Fig. 5a shows sap  
308 velocity data from 09:30 to 12:30 h at 30-min intervals; the vertical strips indicate the periods  
309 when the chamber was closed. Apparently, the sap flow velocity is slightly reduced during and  
310 immediately after the closing. The velocity is then normally recovered few minutes after the  
311 chamber re-opening. Fig. 5b shows the relative decrease in sap flow velocity vs. duration of the  
312 closure. The maximum relative decrease in transpiration rate (15%) occurred for the longest  
313 closure time (400 s). For a normal measurement period of 180 s the maximum decrease was  
314 8%.

315 Fig. 6 details the changes occurring in vapour pressure deficit (VPD), water vapour  
316 concentration and canopy conductance for the longest duration of chamber closure shown in

317 Fig. 5a (400 s, at 11:04 h). The canopy conductance (Eq. (8)) decreases from 2.1 to 1.7 mm s<sup>-1</sup>  
318 (19%), but mainly in the late part of this long clo- sure period: in the first 200 s of chamber  
319 closure G<sub>c</sub> is practically constant.

320 During closure, a decrease 1.2 kPa in VPD occurs, as a conse- quence of the increase of water  
321 vapour concentration from 20.2 to 38.2 mmol mol<sup>-1</sup> . Although not noticeably, the plot of water  
322 vapour concentration is unlinear, due to the effect of gradient reduction. The error in the  
323 calculation of the water vapour flux induced by the use of a linear regression instead than a QR  
324 exceeds 20%, over this long measurement.

325

#### 326 3.4. Adjusted measurement window and minimization of the gradient effect

327 The lag and mixing time measured were always found in the range between 20 and 40 s after  
328 closure; the beginning of the calculation window was assumed 30 s in average. The optimal  
329 duration of the measurement windows was adjusted to 70 s: with that sam- pling duration, the  
330 underestimation of the gas exchange fluxes calculated with the linear regression with respect  
331 to the quadratic method on the 175 field measurement was minimal (3.7% for CO<sub>2</sub> and 5.6% for  
332 water vapour), ensuring that the nonlinearity in the gas concentration data with time had the  
333 less possible impact on the calculation of fluxes.

#### 334 3.5. An example of canopy gas exchange measurements

335 Fig. 7 shows the daily time course of assimilation (A, Fig. 7a), transpiration (E, Fig. 7b), and  
336 canopy conductance (G<sub>c</sub>, Fig. 7c) for two trees on 6 September 2007 when the difference in  
337 water status between the control irrigation (CI) and regulated deficit irriga- tion (RDI) treatments  
338 was maximum. The Plant Leaf Area of the trees resulted: 20.19 m<sup>2</sup> for CI and 26.87 m<sup>2</sup> for RDI.  
339 The total CO<sub>2</sub> net uptakes during the measurement period (from 06:30 to 17:30 h solar time)  
340 were very different: 21.68 and 9.86 g CO<sub>2</sub> m<sup>-2</sup> for CI and RDI trees, respectively. The peak  
341 assimilation rate occurred in the morning, with 2.56 g CO<sub>2</sub> m<sup>-2</sup> h<sup>-1</sup> (CI, at 11:00 h) and 1.33 g  
342 CO<sub>2</sub> m<sup>-2</sup> h<sup>-1</sup> (RDI, at 08:30 h), then it decreased during the afternoon. Transpiration showed a  
343 different diurnal pattern: in the CI it reached its maximum value (0.3 L m<sup>2</sup> ) at 13:00 h, remain-  
344 ing high until late afternoon; on the contrary, in the stressed tree E was relatively flat, reaching  
345 the maximum value in the morning at 10:45 h. The total water transpired by the CI tree during  
346 the day was 2.34 L m<sup>-2</sup> , whereas the stressed RDI tree only lost 0.77 L m<sup>-2</sup> of water over the  
347 same time.

348 The diurnal course of canopy conductance in Fig. 7c was calcu- lated from Eq. (7) (where t (s) is  
349 taken equal to the beginning of the calculation window), using the same gas exchange  
350 measurements shown in Fig. 7a and b. Right after sunrise, the G<sub>c</sub> in the well- irrigated tree  
351 increases steeply with global radiation; the water stressed tree showed the same behaviour,  
352 but to a much lesser extent. The time of maximum G<sub>c</sub> is reached in the RDI treatment first (1.9  
353 mm s<sup>-1</sup> at 07:10 h) than in the well-irrigated CI (5 mm s<sup>-1</sup> at 08:00 h). After reached the peak,  
354 G<sub>c</sub> followed a light decreasing during the daytime period in both trees.

355 Measuring CO<sub>2</sub> and water vapour exchange at the same time allows the measurement of the  
356 instantaneous water use efficiency (WUE), i.e. the ratio of assimilated CO<sub>2</sub> per unit transpired

357 water. The water use efficiency of the gas exchange measurements of 6 September 2007 is  
358 presented in Fig. 8, plotted vs. VPD. For both trees WUE show an inverse relation with VPD, with  
359 a curvilinear pattern. The highest plotted values of WUE are early-morning values, with low VPD.  
360 The WUE was higher in the water stressed tree (RDI) than in the control (CI) for all the duration  
361 of the day; the daily values of WUE were 9.25 and 12.74 g CO<sub>2</sub> L<sup>-1</sup> of transpired water for the CI  
362 and RDI trees respectively.

#### 363 **4. Discussion**

364 The large volume of the chamber determines that the relative error associated to CO<sub>2</sub> leakage  
365 flux (0.8% min<sup>-1</sup>) is very small, in particular considering the short time required to obtaining a  
366 measurement. The leakage coefficients (Fig. 2) calculated for each period into which the  
367 experiment was divided show an evident variability (Fig. 2), which is probably a consequence of  
368 the pressure waves induced by wind gusts around the chamber walls (the experiment was  
369 conducted in open air, under field conditions). The leakage error is lower than those reported in  
370 the literature for transient-state closed chambers. Held et al. (1990) calculated a leak flow error  
371 of 4% min<sup>-1</sup> injecting CO<sub>2</sub> into the chamber, from an initial concentration gradient between the  
372 chamber and the ambient air of 50 μmol mol<sup>-1</sup>. Grau (1995), with an open-bottom chamber  
373 inserted on a bed of sterilised sand, evaluated an under-estimation error due to leakage of 5%  
374 in a standard measure with a small (62.5 L) chamber. Steduto et al. (2002) determined a max-  
375 imum relative error of 4% min<sup>-1</sup> for both CO<sub>2</sub> and water vapour, under different gradients of  
376 gas concentrations.

377 The linear relationship (Fig. 3) between the water vapour amounts injected into the chamber  
378 and the ones detected by the IRGA indicated that the chamber is capable to measure correctly  
379 the changes in water vapour concentration. The slope and intercept of the regression line are  
380 not significant, indicating that errors of water vapour absorption on the chambers walls and in  
381 the tubing are either absent or too small to be detectable. This result is not surprising, as  
382 adsorption is expected to be a function of the surface area per unit volume, thus must be low in  
383 large chambers.

384 The attenuation of the global radiation measured under clear-sky conditions (9.9–14.6%) is  
385 similar to those found in literature (Reicosky et al., 1983; Held et al., 1990; Pickering et al.,  
386 1993; Steduto et al., 2002; Dragoni et al., 2005). Pickering et al. (1993) reported that corrections  
387 to transpiration rates appear to be unnecessary for radiation attenuation of 10%.  
388 Nevertheless, according to Held et al. (1990), a simple correction in net CO<sub>2</sub> assimilation may  
389 be applied to the calculated fluxes, once it is known the light response curve of the assimilation  
390 in the canopy under study. The transmittance of the film in the measured wavelengths  
391 exceeded manufacturer's rate (87% for the whole visible spectrum).

392 The maximum recorded increase in canopy temperature during closure (1.3°C min<sup>-1</sup>, Fig. 4) is  
393 significantly lower than those (2–4°C min<sup>-1</sup>) reported in the literature with closed chambers  
394 (McPherson et al., 1983; Reicosky, 1990a, 1990b; Wagner and Reicosky, 1992; Grau, 1995;  
395 Steduto et al., 2002). The large volume of the chamber and the low rate of air temperature  
396 increase (maximum value of 0.7 °C min<sup>-1</sup>) maintains the effectiveness of the convective  
397 cooling for a long time, and the good long-wave transmissivity of the polyester sheet allows an  
398 efficient radiative energy loss.

399 It is not easy to predict a priori the effect of a ventilated chamber over the gas exchange rate of  
400 an enclosed plant. The changes in the concentration of atmosphere gases may have complex  
401 effects on many physiological processes (Bazot et al., 2008). Although many disturbances  
402 generated by the confined atmosphere act toward a rate decrease with respect to the  
403 undisturbed plant in open air, for example the reduction in the leaf-atmosphere gradient or in  
404 the radiation available (Nicolás et al., 2008), some other perturbations may have the opposite  
405 result. For example, in calm conditions, the artificial ventilation may well reduce the boundary  
406 layer thickness of the leaves inside the chamber compared with those outside, thus actually  
407 enhancing the gas exchange rate. The results of the sap velocity experiment proved that this  
408 hypothesis is not true for this chamber: the effect of long exposition to the enclosed  
409 environment always reduced the transpiration rate measured independently, and the reduction  
410 seems directly proportional to the closure duration (Fig. 5a and b). Consequently, the  
411 chamber should be closed during the shortest time possible to avoid underestimation of water  
412 vapour, and – presumably – CO<sub>2</sub> fluxes.

413 Canopy conductance ( $G_c$ ) of olive trees resulted affected by chamber closure to a very small  
414 degree, and only after a closure duration that exceeds by a considerable margin every measure-  
415 ment requirement (Fig. 6). Therefore, the transpiration responded mainly to changes in the  
416 humidity gradient. Unfortunately, we had no independent measurement of CO<sub>2</sub> assimilation  
417 (as we had of transpiration) to explicitly prove that the overall change in the rate of CO<sub>2</sub> flux due  
418 to canopy enclosing is irrelevant. Nevertheless, the relative changes in the leaf/chamber CO<sub>2</sub>  
419 gradient occurring during a measurement are by far smaller than the ones in water vapour  
420 concentration, thus, as  $G_c$  is almost constant, the changes in assimilation (or respiration)  
421 rates induced by the chamber must be very small.

422 The optimal duration of the calculation window should be at the same time: (a) long enough to  
423 allow an adequate absolute gas concentration increase that minimise the error in the flux  
424 calculation; and (b) short enough to induce the lesser possible nonlinearity in the gas  
425 concentration vs. time. The nonlinearity in the gas concentration vs. time within a single  
426 closure operation can be taken as a measure of the disturbance inflicted to the system. In a  
427 given chamber, this nonlinearity depends not only on the closure time, but also on the actual  
428 gas exchange rate of the canopy under study. The analysis conducted comparing quadratic and  
429 linear regression fits under very different conditions suggest that nonlinearity is almost  
430 unavoidable at high gas exchange rate, but still it is extremely small with 180 s closing time. We  
431 established that 100 s (30 s of lag and stirring time plus 70 s of calculation window) is an  
432 optimal closure time for the chamber presented here.

433 The relationship between hourly WUE and VPD in a well-irrigated olive, presented in Fig. 8 is  
434 very similar to those measured by Moriana et al. (2002) with a leaf cuvette and by Testi et al.  
435 (2008) with eddy covariance measurements. The WUE in the RDI tree was higher than the one of  
436 CI: stomatal closure (Fig. 7c) under stress is a behaviour aimed to reduce the cost of carbon in  
437 terms of water used.

## 438 **5. Conclusions**

439 (1) This work demonstrated that it is possible to measure the CO<sub>2</sub> and water vapour exchange  
440 rates of whole canopies up to 20–30 m<sup>3</sup> by a large closed chamber of the transient-state type.

441 (2) The large chamber volume reduced the impact of the main sources of error in calculating the  
442 gas exchange flux in this type of chambers, namely: leakage, adsorption, canopy, air heating,  
443 and leaf/air gradient reduction.

444 (3) Field tests showed that this chamber imposes minimum dis- turbance on the canopy  
445 environment, and that no appreciable alteration in canopy conductance is generated during  
446 standard measurements.

447 (4) The minimum time required before the measurements of gas concentration can be used to  
448 calculate the gas exchange rate has been estimated in 30 s (lag and mixing time). The optimal  
449 duration for a measurement period with minimum disturbance on the canopy was estimated in  
450 70 s.

451 (5) The concurrent sap flow measurements allowed to quantify the effect of the chamber  
452 closure on the transpiration rate. Enclos- ing the canopy reduced slightly the sap velocity,  
453 proportionally to the closing duration. Under normal measurement condition, with closure  
454 durations between 100 and 180 s, the transpira- tion at the time of re-opening should be  
455 reduced by less than 5%. It should be emphasised that this underestimation is only a potential  
456 disturbance; it will not affect the gas exchange mea- surements when the calculations are  
457 made with the quadratic method (where the rate is taken from the slope at the beginning of the  
458 calculation window).

459 (6) The field measurements on trees in different water conditions yielded results that are in  
460 accordance with the literature.

461 (7) The minimal effects that the chamber generated over the physiological processes of the  
462 enclosed tree indicate that this chamber design is suitable for accurate measures of gas  
463 exchange at tree level in almost all the cultivated fruit trees.

#### 464 **Acknowledgements**

465 This work was funded by projects AGL-2004-05717 of Ministe- rio de Educación y Ciencia of  
466 Spain and P08-AGR-4202 of Junta de Andalucía. We appreciate the contribution of Mr. Rafael  
467 del Río and Mr. Ignacio Calatrava for measurements and technical support of the chambers in  
468 the field campaign.

#### 469 **References**

470 Bazot, S., Blum, H., Robin, C., 2008. Nitrogen rhizodeposition assessed by a  $^{15}\text{NH}_3$  shoot  
471 pulse-labelling of *Lolium perenne* L. grown on soil exposed to 9 years of  $\text{CO}_2$  enrichment.  
472 *Environmental and Experimental Botany* 63, 410–415.

473 Denmead, O.T., 1984. Plant physiological methods for studying evapotranspiration: problems  
474 of telling the forest from the trees. *Agricultural Water Management* 8 (1–3), 167–189.

475 Denmead, O.T., Dunin, F.X., Wong, S.C., Greenwood, E.A.N., 1993. Measuring water use  
476 efficiency of Eucalypt trees with chambers and micrometeorological tech- niques. *Journal of*  
477 *Hydrology* 150 (2–4), 649–664.

478 Dugas, W.A., Fitschen, L.J., Held, A.A., Matthias, A.D., Reicosky, D.C., Steduto, P., Steiner, J.L.,  
479 1991. Bowen ratio, eddy correlation, and portable chamber measure- ments of sensible and  
480 latent heat flux over irrigated spring wheat. *Agricultural and Forest Meteorology* 56, 1–20.

481 Dragoni, D., Lakso, A.N., Piccioni, R.M., 2005. Transpiration of apple trees in a humid climate  
482 using heat pulse sap flow gauges calibrated with whole-canopy gas exchange chambers.  
483 *Agricultural and Forest Meteorology* 130 (1–2), 85– 94.

484 Grau, A., 1995. A closed chamber technique for field measurement of gas exchange of forage  
485 canopies. *New Zealand Journal of Agricultural Research* 38, 71–77. Greenwood, E.A.N.,  
486 Beresford, J.D., Bartle, J.R., 1981. Evaporation from vegetation in  
487 landscapes developing secondary salinity using the ventilated-chamber tech- nique. III.  
488 Evaporation from a *Pinus radiata* tree and the surrounding pasture in an agroforestry plantation.  
489 *Journal of Hydrology* 50, 155–166.

490 Held, A.A., Steduto, P., Orgaz, F., Matista, A., Hsiao, T.C., 1990. Bowen ratio/energy balance  
491 technique for estimating crop net CO<sub>2</sub> assimilation, and comparison with a canopy chamber.  
492 *Theoretical and Applied Climatology* 42, 203–213.

493 Jarvis, P.G., Catsky, J., Eckart, T.E., Koch, D., Koller, D., 1971. General principles of gaso-  
494 metric methods and the main aspects of installation design. In: Sestak, Z., Catsky, J., Jarvis, P.G.  
495 (Eds.), *Plant Photosynthesis Production: Manual of Methods*. Dr. W. Junk N. V. Publishers, The  
496 Hague, pp. 49–110.

497 Leuning, R., Foster, I.J., 1990. Estimation of transpiration by single trees: compari- son of a  
498 ventilated chamber, leaf energy budgets and a combination equation. *Agricultural and Forest*  
499 *Meteorology* 51 (1), 63–86.

500 McLeod, M.K., Daniel, H., Faulkner, R., Murison, R., 2004. Evaluation of a enclosed portable  
501 chamber to measure crop and pasture actual evapotranspiration at small scale. *Agricultural*  
502 *Water Management* 67, 15–34.

503 McPherson, H.G., Green, A.E., Rollinson, P.L., 1983. The measurement, within seconds, of  
504 apparent photosynthetic rates using a portable instrument. *Pho- tosynthetica* 17, 395–406.

505 Meyer, W.S., Reicosky, D.C., Barrs, H.D., Shell, G.S.G., 1987. A portable chamber for measuring  
506 canopy gas-exchange of crops subject to different root zone condi- tions. *Agronomy Journal* 79,  
507 181–184.

508 Moriana, A., Villalobos, F.J., Fereres, E., 2002. Stomatal and photosynthetic responses of olive  
509 leaves to water deficits. *Plant, Cell and Environment* 25, 395–405.

510 Nicolás, E., Barradas, V.L., Ortun ò, M.F., Navarro, A., Torrecillas, A., Alarcón, J.J., 2008.  
511 Environmental and stomatal control of transpiration, canopy conductance and decoupling  
512 coefficient in young lemon trees under shading net. *Environmental and Experimental Botany* 63,  
513 200–206.

514 Orgaz, F., Villalobos, F.J., Testi, L., Fereres, E., 2007. A model of daily mean canopy con-  
515 ductance for calculating transpiration of olive canopies. *Functional Plant Biology* 34, 178–188.

516 Pickering, N.B., Jones, J.W., Boote, K.J., 1993. Evaluation of portable chamber tech-  
517 nique for measuring canopy gas exchange by crops. *Agricultural and Forest Meteorology* 63, 239–254.

518 Reicosky, D.C., Peter, D.B., 1977. A portable chamber for rapid evapotranspiration  
519 measurements on field plots. *Agronomy Journal* 69, 729–732.

520 Reicosky, D.C., Sharrat, B.S., Ljungkull, J.E., Barker, D.G., 1983. Comparison of alfalfa  
521 evapotranspiration measured by weighing lysimeter and portable chamber. *Agricultural*  
522 *Meteorology* 28, 205–211.

523 Reicosky, D.C., Wagner, S.W., Devine, O.J., 1990. Methods of calculating carbon diox-  
524 ide  
525 exchange rates for maize and soybean using a Portable Field Chamber. *Photosynthetica* 24 (1),  
22–38.

526 Reicosky, D.C., 1990a. Canopy gas exchange in the field: closed chambers. *Remote Sensing*  
527 *Reviews* 5 (1), 163–177.

528 Reicosky, D.C., 1990b. A portable chamber for evapotranspiration measurements and irrigation  
529 scheduling. *Acta Horticulturae* 278, 455–461.

530 Steduto, P., Cetinkökü, Ö., Albrizio, R., Kanber, R., 2002. Automated closed-system canopy-  
531 chamber for continuous field-crop monitoring of CO<sub>2</sub> and H<sub>2</sub>O fluxes. *Agricultural and Forest*  
532 *Meteorology* 111, 171–186.

533 Testi, L., Orgaz, F., Villalobos, F.J., 2008. Carbon exchange and water use efficiency of a  
534 growing, irrigated olive orchard. *Environmental and Experimental Botany* 63, 168–177.

535 Testi, L., Villalobos, F.J., 2009. New approach for measuring low sap velocities in trees.  
536 *Agricultural and Forest Meteorology* 49, 730–734.

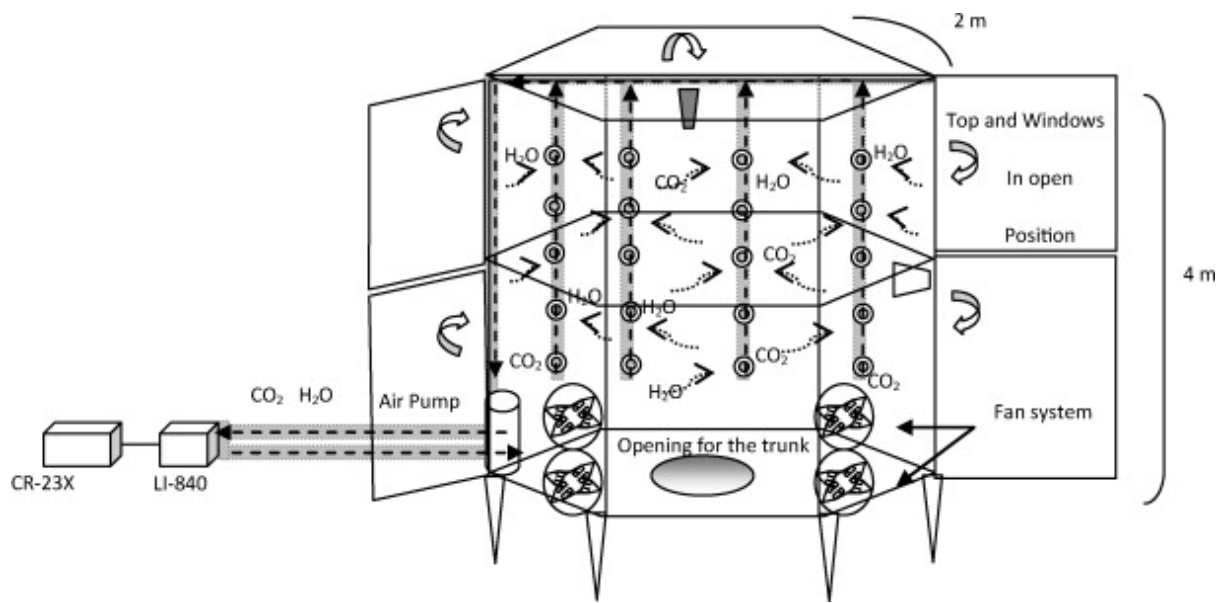
537 Villalobos, F.J., Orgaz, F., Testi, L., Fereres, E., 2000. Measurement and modeling of  
538 evapotranspiration of olive (*Olea europaea* L.) orchards. *European Journal of Agronomy* 13,  
539 155–163.

540 Wagner, S.W., Reicosky, D.C., 1992. Closed-chamber effects on leaf temperature, canopy  
541 photosynthesis, and evapotranspiration. *Agronomy Journal* 84 (4), 731–738.

542 Wagner, S.W., Reicosky, D.C., Saamuel Alessi, R., 1997. Regression models for cal-  
543 culating  
gas fluxes measured with a closed chamber. *Agronomy Journal* 89, 279–284.

544

545 **List of figures**

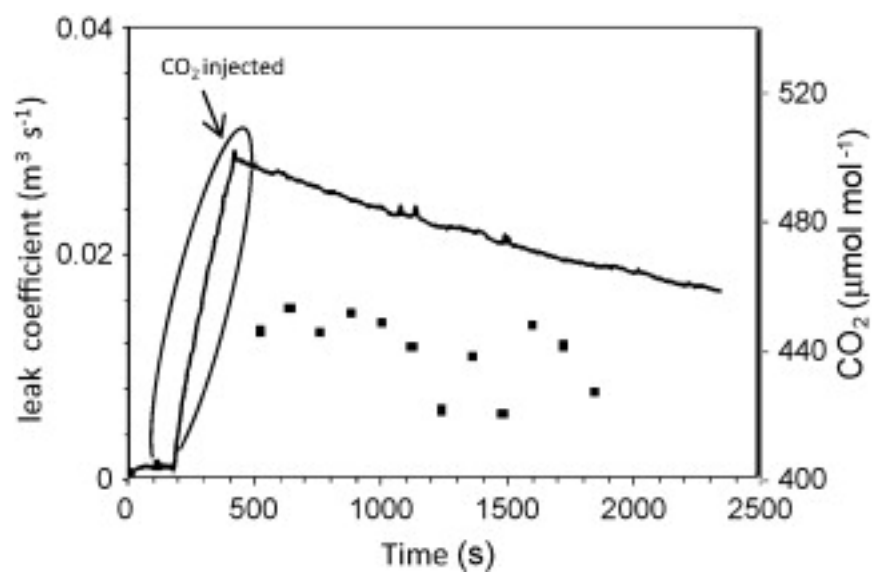


546

547 Fig. 1. Schematic drawing of the chamber, showing the opening windows and other  
548 components. The arrows indicate the air flow through the sampling circuit, and its return to  
549 the chamber.

550

551

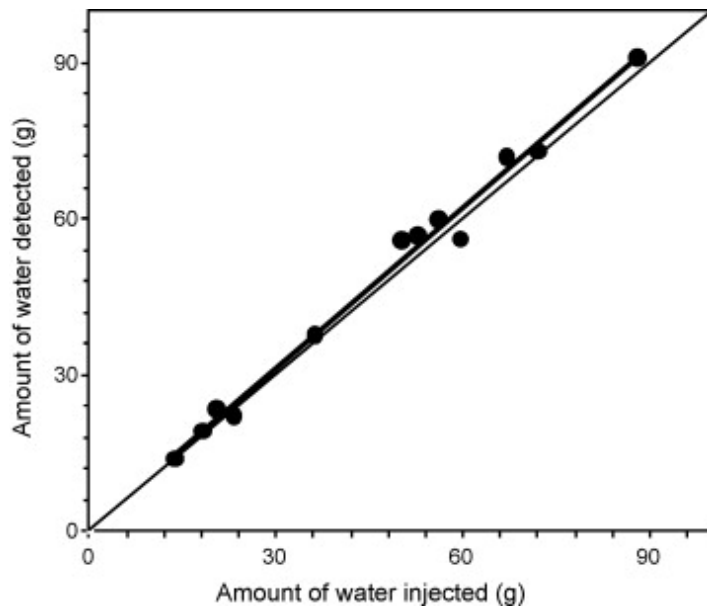


552

553 Fig. 2. Leakage test: the decline in the internal  $\text{CO}_2$  concentration after a  $\text{CO}_2$  injection (solid  
554 line). The squares show the leak coefficients calculated for 2-min intervals. The test yielded a  
555 relative error of  $0.8\% \text{ min}^{-1}$ .

556

557



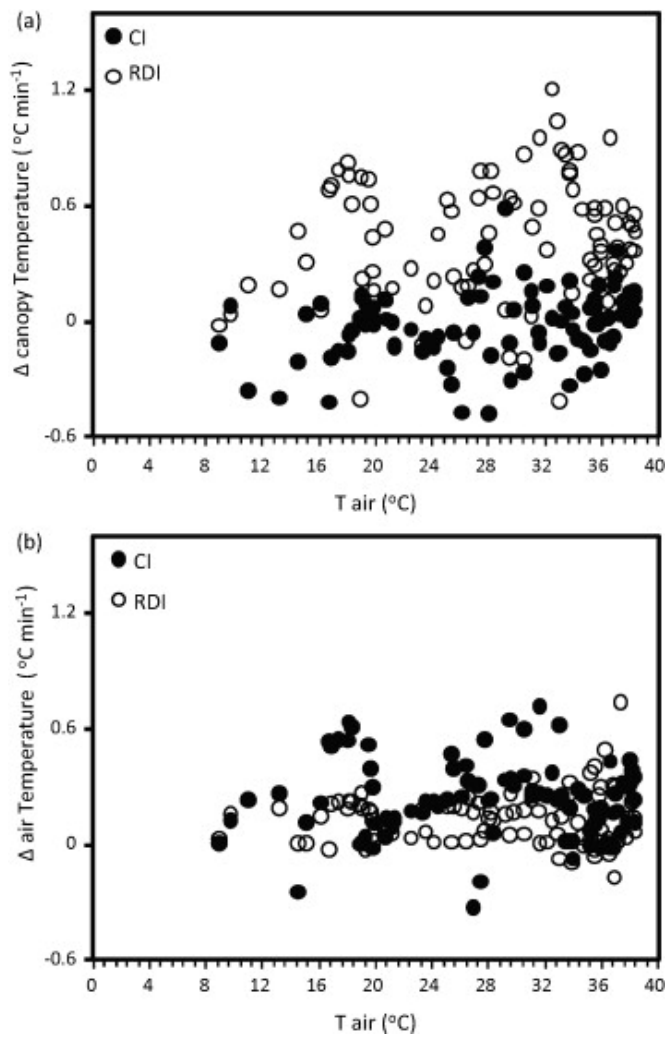
558

559 Fig. 3. Adsorption test and response to a known amount of water vapour, manually injected.

560 The equation of the regression line was:  $y = 1.0295x + 0.5556$  ( $R^2 = 0.99$ ,  $N = 12$ ).

561

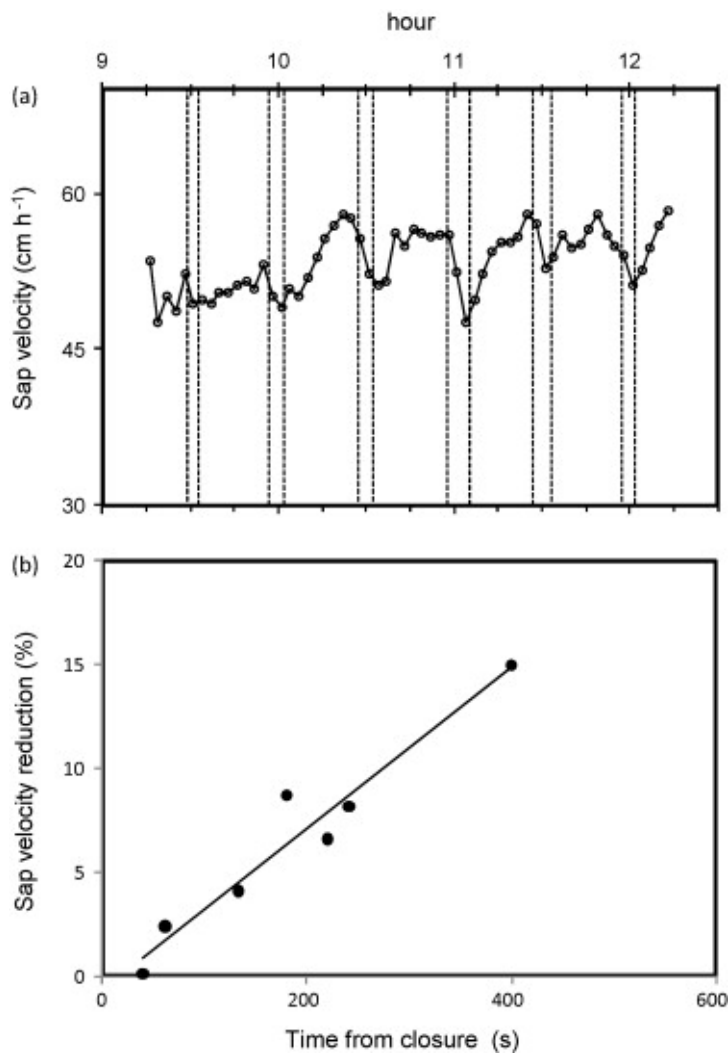
562



563

564 Fig. 4. Increases in canopy temperature (a) and air temperature (b), expressed in  $^{\circ}\text{C}$  increase  
565 per minute since chamber closure, both plotted vs. air temperature outside the chamber.  
566 Measurements taken during 2007 in olive. Black circles: well-irrigated (CI) treatment; white  
567 circles: water stressed (RDI) treatment.

568



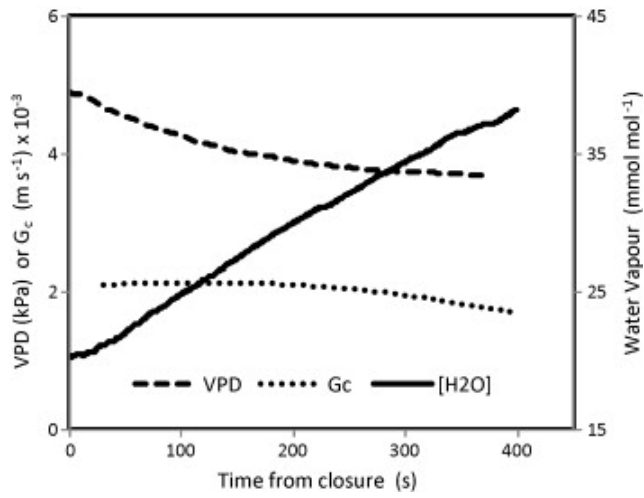
570

571 Fig. 5. (a) Sap velocity measured with compensated heat pulse sap flow probes in an olive  
 572 tree during chamber closure and re-opening. The vertical dashed lines delimit the closure  
 573 periods of different durations (from 252 s (at 09:30 h) to 464 s (at 11:00 h)). (b) Relation  
 574 between time from closure and reduction in sap velocity. The equation of the regression line  
 575 is:  $y = 0.0388x - 0.62$  ( $R^2 = 0.94$ ,  $N = 7$ ).

576

577

578

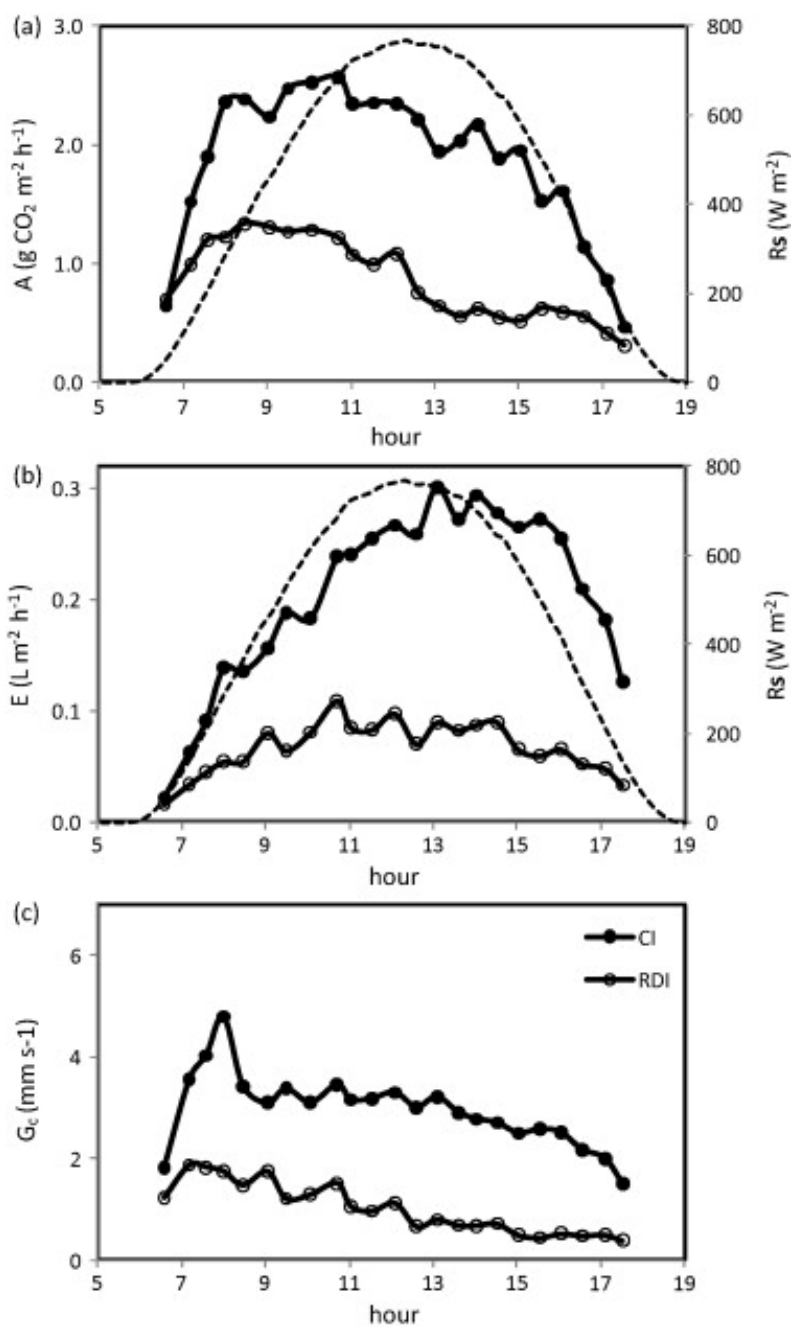


579

580 Fig. 6. Changes recorded in some chamber environment variables during the closure  
581 operation at 11:00 h shown in Fig. 5: vapour pressure deficit (VPD – dashed line), water  
582 vapour concentration ( $[H_2O]$  – solid line) and canopy conductance ( $G_c$  – dotted line).

583

584



586

587 Fig. 7. Diurnal courses of (a) canopy net assimilation; (b) transpiration; and (c) canopy  
 588 conductance in olive trees under different water status, all measured with the gas exchange  
 589 chamber on 6 September 2007. Black circles: well irrigated (CI treatment); white circles:  
 590 water stressed (RDI treatment). The global radiation is also shown (dashed line). Fluxes  
 591 were determined using a calculation window of 70 s.

592

593

